# Low-threshold GaAs/AlGaAs quantum-well lasers grown by organometallic vapor-phase epitaxy using trimethylamine alane

W. S. Hobson, J. P. van der Ziel, A. F. J. Levi, J. O'Gorman, and C. R. Abernathy
*AT&T Bell Laboratories, Murray Hill, New Jersey 07974*

M. Geva, L. C. Luther, and V. Swaminathan
*AT&T Bell Laboratories, Breinigsville, Pennsylvania 18031*

(Received 18 January 1991; accepted for publication 25 March 1991)

We have utilized a new aluminum source, trimethylamine alane (TMAA), in the growth of graded-index separate-confinement heterostructure single quantum-well GaAs/AlGaAs laser structures by low pressure (30 Torr) organometallic vapor-phase epitaxy. We find lower carbon and oxygen incorporation in AlGaAs epilayers using TMAA since it does not contain a direct Al–C bond and it is not susceptible to the formation of volatile Al–O containing compounds. The oxygen and carbon concentrations were below the detection limits ($< 5 \times 10^{16}$ cm$^{-3}$ and $< 3 \times 10^{16}$ cm$^{-3}$, respectively) of the secondary ion mass spectrometry measurements. Broad-area lasers with 10-nm quantum wells and $Al_{0.45}Ga_{0.55}As$ cladding layers exhibited threshold current densities of 140 A cm$^{-2}$ for cavity lengths of 1 mm, internal quantum efficiencies of 81%, and intrinsic losses of 1.6 cm$^{-1}$. These results demonstrate that extremely high-quality AlGaAs and GaAs quantum wells can be grown with TMAA.

## I. INTRODUCTION

There is considerable interest in exploring alternative precursors for organometallic vapor-phase epitaxy (OMVPE) and metalorganic molecular-beam epitaxy (MOMBE). Some of the motivations include improving process safety, reducing the incorporation of intrinsic impurities (e.g., carbon) associated with the organometallic source, and decreasing the susceptibility of the source to contamination with extrinsic impurities (e.g., oxygen). A particularly promising aluminum precursor which addresses each of these issues is trimethylamine alane (TMAA), which can exist as either the mono-$(CH_3)_3N{\cdot}AlH_3$, or bis-$[(CH_3)_3N]_2{\cdot}AlH_3$, adduct. TMAA is far less reactive in air than the commonly used Al organometallic precursors such as trimethylaluminum (TMA1) and triethylaluminum (TEA1) which are highly pyrophoric. The synthesis and properties of TMAA have been discussed in several publications.[1–7] Unlike TMA1 and TEA1 there is no direct Al–C bond in TMAA which leads to an expectation of reduced carbon incorporation. In addition, reaction of TMAA with oxygen will result in the formation of involatile Al–O containing compounds such as $Al_2O_3$.[2] This is in sharp contrast to TMA1 and TEA1 which are susceptible to volatile aluminum alkoxide contamination leading to oxygen-contaminated AlGaAs epilayers.[8]

The first use of TMAA for III-V epitaxy was by Abernathy *et al.*[9] They found that high-quality AlGaAs layers could be grown in a MOMBE system with significantly lower oxygen and carbon incorporation compared to the conventional Al sources. High-performance heterojunction bipolar transistors were also fabricated.[10] Hobson *et al.*[11] reported high-quality (i.e., low carbon, intense photoluminescence, featureless surface morphology, and high-purity) AlGaAs grown by low-pressure OMVPE and demonstrated a GaAs/AlGaAs V-groove laser. Other workers have also obtained AlGaAs with low carbon content by low-pressure OMVPE using TEGa and TMAA, but noted Si contamination from their TMAA source ($N_D$-$N_A$ of $7.4 \times 10^{15}$ cm$^{-3}$ for $Al_{0.31}Ga_{0.69}As$ and $1.2 \times 10^{16}$ cm$^{-3}$ for $Al_{0.49}Ga_{0.51}As$).[12]

We report here on the growth of AlGaAs using TMAA and the device characterization of broad-area graded-index separate-confinement heterostructure single quantum-well (GRIN-SCH SQW) lasers. This device structure serves as a test of the optical quality of the AlGaAs grown with TMAA and of the ability to produce high-quality GaAs/AlGaAs interfaces. Low thresholds ($J_{th} = 140$ A/cm$^2$ for 1-mm cavity length) and very low total internal losses ($\alpha_i = 1.6$ cm$^{-1}$) demonstrate the utility of TMAA for the growth of high-quality optical materials.

## II. CRYSTAL GROWTH

A low-pressure (30 Torr) vertical OMVPE reactor was used for the growth of the GRIN-SCH SQW laser structures in a reactor design described previously.[13] The hydrogen carrier gas flow was 6.51 min$^{-1}$, resulting in a gas velocity greater than 1.0 m s$^{-1}$. This was found to be necessary in order to minimize decomposition of TMAA upstream of the wafer. No visible coating could be observed on the quartz wall even after several growth runs. The gallium source was TEGa and arsine was used as the arsenic source. Constant mass flow rates of $4.4 \times 10^{-3}$ mol min$^{-1}$ for $AsH_3$ and $1.3 \times 10^{-5}$ mol min$^{-1}$ for TEGa were utilized. The resultant GaAs growth rate was 210 nm min$^{-1}$. Graded AlGaAs layers were obtained by varying the TMAA flow in steps to give an approximately linear variation in Al mole fraction. The TMAA bubbler

 0021-8979/91/010432-04$03.00  

TABLE I. Epitaxial layer structure of GRIN-SCH SQW laser.

| Al mole fraction ($Al_xGa_{1-x}As$) | Thickness (nm) | Doping concentration ($p,n$: $10^{18}$ cm$^{-3}$) |
|---|---|---|
| $x=0$ | 200 | $p=40$ |
| $x=0.45\rightarrow 0$ | 100 | $p=5$ |
| $x=0.45$ | 1600 | $p=1.5$ |
| $x=0.2\rightarrow 0.45$ | 230 | $p=0.2$ |
| $x=0.2$ | 15 | ... |
| $x=0$ | 10 | ... |
| $x=0.2$ | 15 | ... |
| $x=0.45\rightarrow 0.2$ | 230 | $n=0.1$ |
| $x=0.45$ | 1600 | $n=0.8$ |
| $x=0\rightarrow 0.45$ | 100 | $n=3$ |
| $x=0$ | 800 | $n=3$ |

was maintained at 19.0 °C and operated at 300 Torr. A TMAA mass flow rate of $1.7 \times 10^{-5}$ mol min$^{-1}$ resulted in an Al mole fraction of 0.45. The TMAA mass flow rate was calculated based on assuming equilibrium between the $H_2$ carrier gas (98 cm$^3$ min$^{-1}$) and the solid TMAA, and using a value of 1.13 Torr as the TMAA vapor pressure at 19.0 °C.[14] Disilane was employed for $n$-type Si doping and diethylzinc (DEZn) for $p$-type Zn doping. No difficulty was observed for Si doping, but a slight yellow-orange deposit was noted on the tip of the quartz flow modifier during the course of Zn doping. A high mass flow rate of $7 \times 10^{-6}$ mol min$^{-1}$ of DEZn was used for the $p^+$ doping, and consequently some prereaction may be occurring. The growth temperature was 700 °C except for the $p^+$ GaAs contact layer, which was grown at 620 °C in order to enhance the Zn incorporation.

## III. RESULTS AND DISCUSSION

The epitaxial layer structure of the GRIN-SCH SQW laser is given in Table I. The confinement layers were intentionally doped while the 10-nm QW and adjacent 15-nm $Al_{0.2}Ga_{0.8}As$ barrier layers were undoped. The laser structures were grown on low-dislocation Si-doped $n^+$-GaAs substrates oriented 2° off (100) toward the nearest (110). Featureless surface morphology was observed by Nomarski differential interference microscopy (1000 ×) for the device layers. Several $Al_xGa_{1-x}As$ calibration layers ($0.1 \leqslant x \leqslant 1$) were grown and characterized. All layers exhibited excellent surface morphology. Double-crystal x-ray diffraction measurements revealed narrow linewidths, with full-width at half maxima typically 2–5 arcsec broader than the corresponding GaAs substrate. AlGaAs layers with direct band gaps ($x<0.37$) were found to have intense room-temperature photoluminescence (PL). Low-temperature PL verified that carbon was present only at very low ($\ll 10^{16}$ cm$^{-3}$) concentrations.[13]

Deep-level transient spectroscopy has been used to characterize Si-doped $Al_xGa_{1-x}As$ ($N_D - N_A = 1$–$9 \times 10^{16}$ cm$^{-3}$, $0.2 \leqslant x \leqslant 0.4$). Only the presence of EL2 at very low concentrations ($< 10^{13}$ cm$^{-3}$) as well as the expected $DX$ center was found.[15] All other traps were below $10^{12}$ cm$^{-3}$, again suggesting that AlGaAs grown with TMAA is of very high quality. We are presently examining

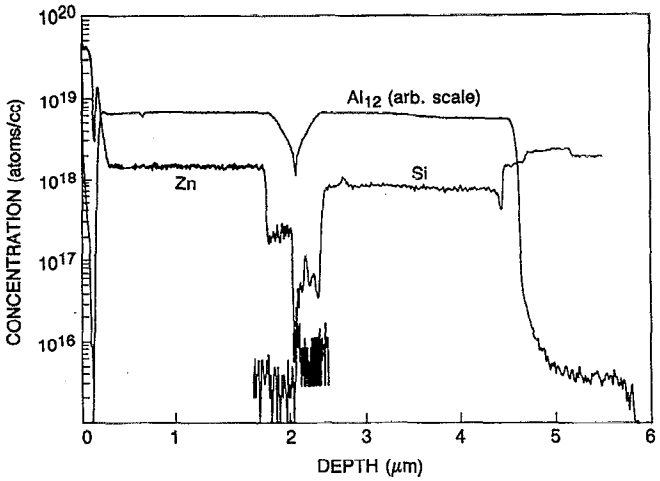


FIG. 1. SIMS profiles of the atomic Al, Zn, and Si concentrations in the GRIN-SCH SQW laser structure.

the PL of quantum wells (QWs) grown under similar conditions to those employed for the GaAs/AlGaAs laser structures.[16] Intense PL at 1.8 K was observed for 10-nm QWs with 50-nm $Al_{0.32}Ga_{0.68}As$ barriers. Growth temperatures of 650 and 700 °C were utilized. The full width at half maximum (FWHM) of the PL peak was 2.5 meV for the sample grown at 650 °C and 4.0 meV for the one at 700 °C. These values are smaller than typically obtained from QWs grown by OMVPE. For example, Schmitz *et al.*[17] reported a FWHM of 6.7 meV for a 10-nm QW with $Al_{0.3}Ga_{0.7}As$ barriers, and Moshevskii *et al.*[18] obtained a value of 6.4 meV for nominally the same structure.

The GRIN-SCH SQW layer structures were characterized by secondary ion mass spectrometry (SIMS) on a CAMECA IMS-4F SIMS instrument. Atomic profiles for Al, Zn, Si, C, and O were obtained. Implants of known doses of the above elements in GaAs and AlGaAs were used for the conversion of the secondary ion counts into the atomic concentration. The depth scale was found by measuring the depth of the sputtered crater subsequent to the analysis. The SIMS profiles for atomic concentrations of Al, Zn, and Si in the GRIN-SCH SQW structure are given in Fig. 1. The linear grading of the AlGaAs graded confinement layers is well defined. The active layer is undoped and the Zn and Si profiles are quite sharp near the QW. The oxygen and carbon levels (not shown) are below the detection limit of the SIMS in this analysis, $< 5 \times 10^{16}$ cm$^{-3}$ and $< 3 \times 10^{16}$ cm$^{-3}$, respectively. This very low value of oxygen is quite encouraging, and is lower than the published values of AlGaAs grown by molecular-beam epitaxy (MBE) where the lowest oxygen levels for $Al_xGa_{1-x}As$ ($0.3 < x < 0.4$) were $4 \times 10^{17}$ cm$^{-3}$.[19] These authors found oxygen at (1.4–1.9) $\times 10^{17}$ cm$^{-3}$ for comparison AlGaAs grown by liquid-phase epitaxy or OMVPE using TMA1. The lowest values of oxygen obtained for AlGaAs grown by MBE and OMVPE using TMA1 for the same SIMS equipment used here were $1 \times 10^{17}$ cm$^{-3}$ and $2 \times 10^{17}$ cm$^{-3}$, respectively.[20]

The laser properties were obtained using wide stripe

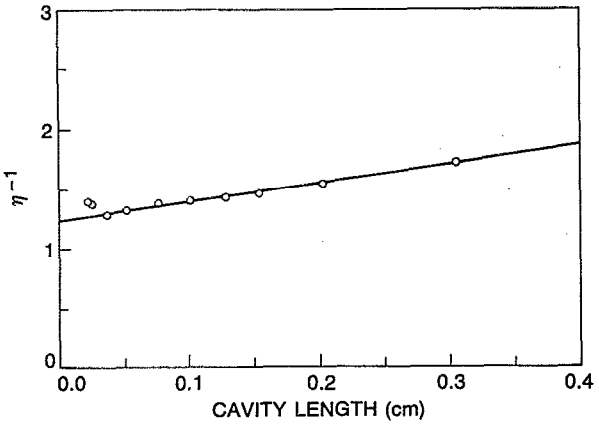


FIG. 2. Inverse differential quantum efficiency as a function of cavity length for the GRIN-SCH SQW laser.

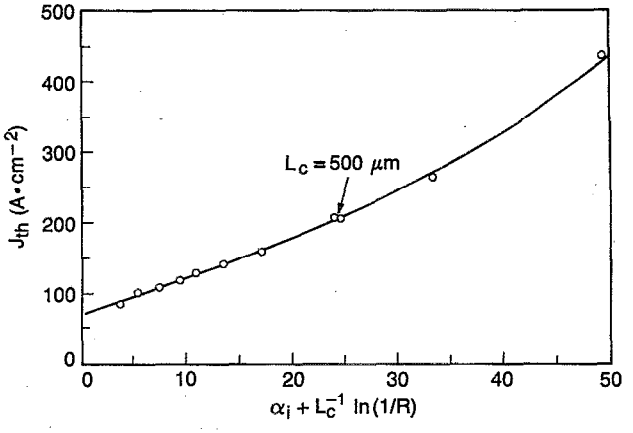


FIG. 3. Threshold current density as a function of inverse cavity length.

ridge lasers. Utilizing standard photolithographic lift off, BeAu/Au stripes from 40 to 120 $\mu$m wide in 20-$\mu$m increments were deposited on the $p$ contact. In order to reduce the current spreading the $p$-GaAs contact layer and approximately half of the $p$-$Al_{0.45}Ga_{0.55}As$ cladding layer was etched away in the region outside of the metal stripes. Au/Sn/Au metals formed the $n$ contact. The light output versus pulsed current dependence was measured as a function of stripe width for several laser lengths $L_c$. For a given laser length, the threshold current is a linear function of stripe width. The slope of the curve yields the threshold current density and the zero stripe width limit yields the current spreading. The external quantum efficiency is independent of stripe width.

The cavity length dependence of the quantum efficiency $\eta$ is given by

$$\eta^{-1}=\eta_i^{-1}[1+\alpha_i L_c/\ln(1/R)], \tag{1}$$

where $\eta_i$ is the internal quantum efficiency, $\alpha_i$ is the internal loss, and $R = \sqrt{R_1 R_2}$ where $R_1$ and $R_2$ are the two facet reflectivities.[21] The experimental values are shown as the open circles in Fig. 2. The value of $\alpha_i$, obtained from the slope of the linear fit, shown by the solid line, is 1.6 cm$^{-1}$. The value of $\eta_i = 0.81$ is obtained from the zero cavity length limit. The value of $\eta_i$ is highly sensitive to the data points for short cavity length. We show below that for cavity lengths shorter than 500 $\mu$m the threshold current, due to band filling, rises more rapidly than the linear dependence obtained for longer cavity lengths. A small decrease in quantum efficiency for the short lasers, associated with the nonlinear threshold current dependence, appears to explain the relatively low internal quantum efficiency.

The threshold current density plotted as a function of $\alpha_i + L_c^{-1}\ln(1/R)$ is given in Fig. 3. For a linear gain/current relationship, the dependence of $J_{th}$ on $L_c$ is

$$J_{th}=J_t+\frac{e}{\Gamma\tau\beta}\left[\alpha_i+\frac{\ln(1/R)}{L_c}\right], \tag{2}$$

where $J_t$ is the transparency current, $\Gamma$ is the optical confinement factor, $e$ is the electronic charge, $\tau$ is the electron lifetime, and $\beta$ is the gain coefficient. A linear relationship of $J_{th}$ on $L_c^{-1}$ holds for $L_c > 500$ $\mu$m. For $L_c < 500$ $\mu$m, $J_{th}$ rises superlinearly with $L_c^{-1}$. In quantum-well lasers the differential gain decreases with increasing carrier density in the well and the nonradiative losses, from the Auger effect and carrier leakage, increases.[22–25] Extrapolation of the $J_{th}$ vs $L_c^{-1}$ data to $L_c^{-1} = 0$, using the linear portion of the curve, yields $J_t = 70$ A/cm$^2$.

The threshold current density is 140 A cm$^{-2}$ for $L_c = 1000$ $\mu$m and 210 A cm$^{-2}$ for $L_c = 500$ $\mu$m and are smaller than obtained for OMVPE-grown GaAs/AlGaAs GRIN-SCH SQW lasers using TMA1 as the Al source. For example, Wagner *et al.* have studied a variety of GRIN-SCH structures grown by OMVPE and obtained the lowest $I_{th}$ of 222 A cm$^{-2}$ at $L_c = 1200$ $\mu$m for a 5-nm QW with a $Al_{0.3}Ga_{0.7}As$ barrier and $Al_{0.6}Ga_{0.4}As$ cladding layer.[26]

Figure 4 shows the dependence of the emission wavelength on cavity length. The shift to shorter wavelength is attributed to band filling of the quantum wells caused by the higher threshold current densities of the shorter lasers. The shift is largest for lasers shorter than 500 $\mu$m which also exhibit a nonlinear $J_{th}$.

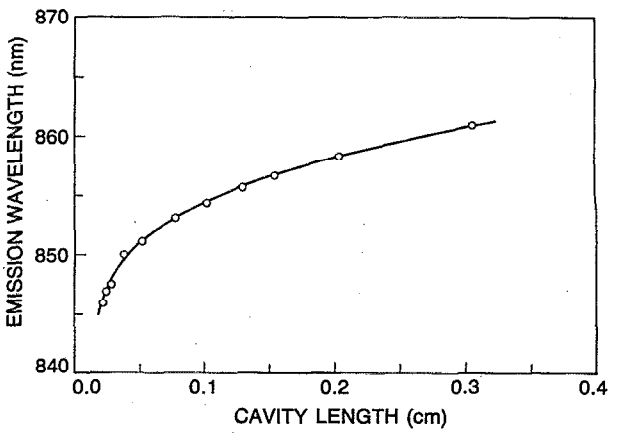


FIG. 4. Lasing emission wavelength as a function of cavity length.

The use of TMAA has several advantages over TMA1 for the growth of AlGaAs with low carbon and oxygen as the growth pressure is reduced. For the case of TMA1, it is desirable to utilize *in situ* reactions which getter volatile aluminum alkoxides. Kuech *et al.*[27] utilized a long reaction inlet section in order to enhance upstream gettering reactions by increasing the residence time and surface area. However, as the growth pressure is lowered and the effective residence time of the precursors is reduced, the probability of gettering reactions decreases. Since TMAA does not contain or form volatile aluminum alkoxides, the requirements of in situ gettering should be reduced. An additional advantage of TMAA over TMA1 at lower pressures is the significantly reduced carbon concentration. In order to decrease the carbon resulting from TMA1, it is necessary to use very high partial pressures of $AsH_3$. For a given total mass flow rate, this is achieved at the expense of increasing the $AsH_3$ flow rate for lower growth pressures in order to maintain the same $AsH_3$ partial pressure.

## IV. CONCLUSIONS

In summary, we have demonstrated that high-quality AlGaAs can be grown by OMVPE at low pressure using TMAA as the aluminum precursor. High-performance GaAs/AlGaAs GRIN-SCH SQW lasers were fabricated, further verifying the ability to produce AlGaAs and GaAs/AlGaAs interfaces of high quality. SIMS analysis showed that oxygen and carbon were present at levels below their detection limits of $5 \times 10^{16}$ cm$^{-3}$ and $3 \times 10^{16}$ cm$^{-3}$, respectively. Low-temperature PL indicates that the residual carbon is well below $10^{16}$ cm$^{-3}$. TMAA will be a useful source for low-pressure OMVPE where oxygen and carbon contamination can not be tolerated. Both of these impurities are of increasing importance for the conventional organometallic sources as the growth pressure is lowered.

## ACKNOWLEDGMENTS

The authors acknowledge Dr. J. L. Zilko for useful discussions and Dr. W. P. Weiner of American Cyanamid Company for discussions related to the use and properties of trimethylamine alane.

[1] G. W. Fraser, N. N. Greenwood, and B. P. Straughan, J. Chem. Soc. 3742 (1963).
[2] C. W. Heitsch, Nature **195**, 995 (1962).
[3] R. A. Kovar and J. O. Callaway, Inorg. Synth. **17**, 36 (1977).
[4] G. N. Nechiporenko, L. B. Petukhova, and A. S. Rozenberg, Izv. Akad. Nauk. SSSR, Ser. Khim. **8**, 1697 (1975).
[5] J. K. Ruff and M. F. Hawthorne, J. Amer. Chem. Soc. **82**, 2141 (1960).
[6] J. K. Ruff, Inorg. Synth. **9**, 30 (1967).
[7] O. Stecher and E. Wiberg, Chem. Ber. **75**, 2003 (1942).
[8] V. Frese, G. K. Regel, H. Hardtdegen, A. Brauers, P. Balk, M. Hostalek, M. Lokai, L. Pohl, A. Miklis, and K. Werner, J. Electron. Mater. **19**, 305 (1990).
[9] C. R. Abernathy, A. S. Jordan, S. J. Pearton, W. S. Hobson, D. A. Bohling, and G. T. Muhr, Appl. Phys. Lett. **56**, 2654 (1990).
[10] F. Ren, C. R. Abernathy, S. J. Pearton, T. R. Fullowan, J. Lothian, and A. S. Jordan, Electron. Lett. **26**, 724 (1990).
[11] W. S. Hobson, A. F. J. Levi, J. O'Gorman, S. J. Pearton, C. R. Abernathy, and V. Swaminathan, Electron. Lett. **26**, 1762 (1990).
[12] A. C. Jones and S. A. Rushworth, J. Cryst. Growth **106**, 253 (1990).
[13] W. S. Hobson, T. D. Harris, C. R. Abernathy, and S. J. Pearton, Appl. Phys. Lett. **58**, 77 (1991).
[14] American Cyanamid Company, Wayne, NJ, Application Note No. 8.
[15] N. G. Paroskevopoulos, S. R. McAfee, and W. S. Hobson (unpublished results).
[16] M. Lamont Schnoes, T. D. Harris, and W. S. Hobson (unpublished results).
[17] D. Schmitz, G. Strauch, J. Knauf, H. Jürgensen, M. Heyen, and K. Wolter, J. Cryst. Growth **93**, 312 (1988).
[18] A. G. Mashevskii, M. A. Sinitsyn, D. R. Stroganov, O. M. Fedorova, and B. S. Yavich, Sov. Tech. Phys. Lett. **14**, 532 (1988).
[19] T. Achtnick, G. Burri, and M. Ilegems, J. Vac. Sci. Technol. **A7**, 2537 (1989).
[20] M. Geva (unpublished results).
[21] G. H. B. Thompson, *Physics of Semiconductor Laser Devices* (J. Wiley & Sons, Chichester, 1980), pp. 96–98.
[22] S. S. Ou, J. J. Yang, J. Z. Wilcox, and M. Jansen, Electron. Lett. **24**, 952 (1988).
[23] J. Z. Wilcox, G. L. Peterson, S. Ou, J. J. Yang, M. Jansen, and D. Schechter, Electron. Lett. **24**, 1218 (1988).
[24] A. R. Reisinger, P. S. Zory, and R. G. Waters, IEEE J. Quant. Electron. **QE-33**, 993 (1987).
[25] P. S. Zory, A. R. Reisinger, L. J. Mawst, G. Costrini, C. A. Zmudzinski, M. A. Emanuel, M. E. Givens, and J. J. Coleman, Electron. Lett. **22**, 475 (1986).
[26] D. K. Wagner, R. G. Waters, P. L. Tihanyi, D. S. Hill, A. J. Roza, H. J. Vollmer, and M. M. Leopold, IEEE J. Quant. Electron. **24**, 1258 (1988).
[27] T. F. Kuech, D. J. Wolford, E. Veuhoff, V. Deline, P. M. Mooney, R. Potemski, and J. Bradley, J. Appl. Phys. **62**, 632 (1987).